Electronic structure of $Gd_5(Si, Ge)_4$

2002 J. Phys.: Condens. Matter 14 7273

(http://iopscience.iop.org/0953-8984/14/30/316)

INSTITUTE OF PHYSICS PUBLISHING JOURNAL OF PHYSICS: CONDENSED MATTER

J. Phys.: Condens. Matter **14** (2002) 7273–7286 PII: S0953-8984(02)36197-6

Electronic structure of $Gd_5(Si, Ge)_4$

G Skorek[1], J Deniszczyk[1,2] and J Szade[1]

[1] A Chelkowski Institute of Physics, University of Silesia, Uniwersytecka 4, 40-007 Katowice, Poland
[2] Institute of Physics and Chemistry of Metals, University of Silesia, Uniwersytecka 4, 40-007 Katowice, Poland

Received 24 April 2002
Published 17 July 2002
Online at stacks.iop.org/JPhysCM/14/7273

Abstract

The electronic structure of the compounds $Gd_5(Si, Ge)_4$ has been investigated with the use of x-ray and ultraviolet photoelectron spectroscopies. The results are compared with calculations performed with the tight-binding linear muffin-tin orbital method for Gd_5Si_4 and Gd_5Ge_4. Very good agreement with the experimental data has been obtained and conclusions about the character of the electronic states, their hybridization and their influence on magnetic and electrical properties have been drawn. The effect of Ti substitution (5 at.%) for Si or Ge in $Gd_5(Si, Ge)_4$ has been investigated. Significant changes in the electronic structure near the Fermi level have been found especially for Gd_5Si_4.

1. Introduction

Compounds of the $Gd_5(Si_xGe_{1-x})_4$ type have been intensively investigated in recent years due to the interesting magnetic behaviour and giant magnetocaloric effect (GMCE) found in $Gd_5Si_2Ge_2$ and compounds with similar stoichiometry [1–3]. Recently, Levin *et al* [4] reported unusual spontaneous generation of voltage accompanying the phase transformation which takes place at the temperature of the GMCE. In an earlier paper we discussed the variation of the photoemission valence band spectra of $Gd_5(Si_xGe_{1-x})_4$ for $x = 0$, 1 and 0.5 [5]. The differences in the spectra, in the binding energy (BE) region close the Fermi level, have been related to the magnetic and electrical properties. Gd_5Si_4 is a ferromagnet with $T_C = 336$ K and $\theta_P = 349$ K (θ_P: paramagnetic Curie temperature) whereas Gd_5Ge_4 orders antiferromagnetically at $T_N = 115$ K and ferromagnetically at $T_C = 20$ K. Very recently, Levin *et al* [6] have reported a magnetic phase diagram for Gd_5Ge_4 and found that the low-temperature magnetic transition AFM–FM is accompanied by a crystallographic one. Moreover, the electrical resistivity of Gd_5Ge_4 shows an unusual transition from metallic behaviour for temperatures below the Néel temperature (130 K) to semiconductor-like behaviour for higher temperatures [5, 6]. Additionally, the calculated electronic structure has been discussed in relation to the magnetic and crystallographic transitions. Gd_5Si_4 and Gd_5Ge_4 crystallize in the Sm_5Ge_4-type orthorhombic structure, with space group *Pnma*. However, Morellon *et al* [7]

have reported that these compounds have two different kinds of *Pnma* orthorhombic structure and the main difference is related to the various inter-atomic distances. The GMCE has been observed at temperatures where the transition from the ferromagnetic orthorhombic to the high-temperature paramagnetic monoclinic structure takes place. For $Gd_5Si_2Ge_2$ the transition has been observed at $T_C = 276$ K in zero magnetic field and T_C has been found to increase with increasing magnetic field [8].

The aim of this contribution is an analysis of the electronic structure of Gd_5Si_4, $Gd_5Si_2Ge_2$ and Gd_5Ge_4. Additionally, $Gd_5Si_{3.8}Ti_{0.2}$ and $Gd_5Ge_{3.8}Ti_{0.2}$ have been investigated. The experimental data have been obtained with the use of x-ray and ultraviolet photoelectron spectroscopy. The temperature dependence of the XPS and UPS spectra in the region of magnetic transitions has also been studied. The experimental data are compared with the results of the electronic structure calculations performed for Gd_5Si_4 and Gd_5Ge_4.

2. Experimental details

The samples of Gd_5Si_4, $Gd_5Si_2Ge_2$, Gd_5Ge_4, $Gd_5Si_{3.8}Ti_{0.2}$ and $Gd_5Ge_{3.8}Ti_{0.2}$ were obtained by the Czochralski method from a levitated melt using gadolinium of 99.9% purity, titanium of 99.99% purity, silicon and germanium of 99.999% purity. The structure was identified by means of x-ray powder diffraction with Cu Kα radiation using the Siemens D-5000 diffractometer. Additionally, the atomic composition of the samples was checked using x-ray photoelectron spectroscopy (XPS) and Auger electron spectroscopy (AES). For $Gd_5Ge_{3.8}Ti_{0.2}$ a slight contamination with GdTiGe in the tetragonal phase was found.

The XPS measurements were performed with a Physical Electronics PHI 5700/660 spectrometer, using monochromatized Al Kα radiation (1486.6 eV). The vacuum during the measurements was about 10^{-10} Torr. The energy resolution was about 0.35 eV. The UPS spectra were obtained using He II radiation (40.8 eV). The samples were fractured or scraped with a diamond file in the UHV chamber just before taking the spectra. For some of them, sputtering with low-energy Ar ions was used to ensure that the surface was free from contaminants.

The electronic structure of Gd_5Ge_4 and Gd_5Si_4 was calculated with the use of the tight-binding linear muffin-tin orbital (TB-LMTO) method in the atomic sphere approximation (TB-LMTO-ASA) [9]. The local spin-density approximation to the exchange–correlation potential in the von Barth–Hedin [10] form with the non-local correction of Langreth, Mehl and Hu [11] was applied. The calculations were scalar relativistic, neglecting the spin–orbit interaction. Only the magnetic solutions were considered. The electronic configurations of the constituent atoms were taken as follows: Gd: $[Xe]4f^7 5d^1 6s^2 6p$, Si: $[Ne]3s^2 3p^2 3d$ and Ge: $[Ar]4s^2 4p^2 4d$. The states of the $3d^{10}$ closed shell of Ge were included in the group of the core states. The crystallographic data were taken from experiment [12].

ASA-based methods demand partitioning of the unit-cell space into Wigner–Seitz (WS) spheres filling up the unit-cell volume. For the Gd_5Ge_4 structure the WS radii were taken in the ranges 3.67–3.92 au for Gd and 2.68–2.82 au for Ge atoms. The Gd_5Si_4 unit cell, though of the same symmetry as that of Gd_5Ge_4, is characterized by different relative positions of constituent atoms. To preserve the reasonably small value of the WS sphere overlap for Gd_5Si_4, sets of WS radii of 3.54–3.88 au for Gd and 2.73–2.85 au for Si atoms were applied. For both sets of WS radii used in the calculations, the total overlap volume was less than 9% (of the unit-cell volume). To reduce the effect of overlapping spheres, the standard combined correction [9] was used in the calculations. The self-consistent calculations were performed with 500 $\boldsymbol{k}$-vectors in the irreducible Brillouin zone (IBZ). Convergence to almost the same values of the total energy and moments of the density of states (DOS) was already achieved for less than 200 $\boldsymbol{k}$-vectors in the IBZ.

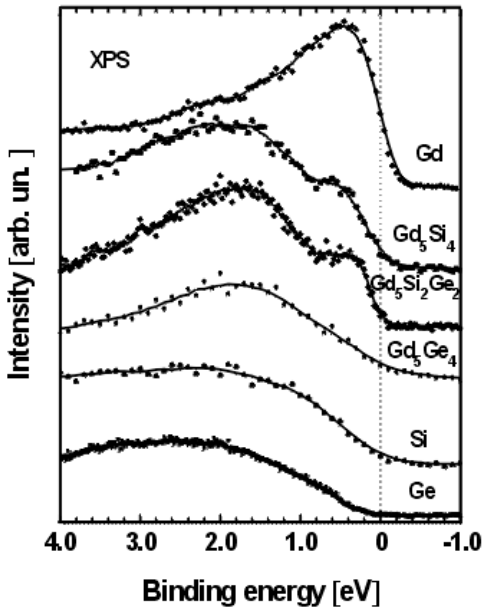

Figure 1. Valence band XPS spectra for Gd_5Si_4, $Gd_5Si_2Ge_2$, Gd_5Ge_4 compounds and Gd, Ge and Si pure elements.

3. Results and discussion

3.1. Experiment

The valence band XPS spectra are presented for BE up to 4 eV for Gd_5Si_4, $Gd_5Si_2Ge_2$ and Gd_5Ge_4 (figure 1). The spectra of the pure elements (Gd, Si, Ge) are added for comparison. The intensities of the spectra of Gd and its compounds are normalized in relation to the Gd 4f photoemission intensity. All $Gd_5(Si, Ge)_4$ compounds show one characteristic feature—a broad maximum at energies 1.5–2 eV, which has been attributed in our earlier paper to the Gd 5d–Si(Ge) sp covalently bonded states [5]. This interpretation is confirmed by our electronic structure calculation, discussed later in the text.

The XPS spectra of Gd_5Si_4, $Gd_5Si_2Ge_2$, Gd_5Ge_4 differ from one another mainly in the BE range 0–1.0 eV. In the spectrum of Gd_5Si_4, a bump is visible at a BE of about 0.7 eV. This feature is shifted closer to the Fermi level by 0.3 eV for $Gd_5Si_2Ge_2$ whereas for Gd_5Ge_4 it is hardly visible. In our earlier paper this effect was discussed in relation to the different magnetic and electrical properties of these compounds. On the other hand, Pecharsky and Gschneidner [12] studied the physical properties on the basis of variation of the numbers and configurations of nearest neighbours in the $Gd_5(Si, Ge)_4$ system. Morellon *et al* [7] have reported that compounds have two different kinds of *Pnma* orthorhombic structure: high-temperature Gd_5Ge_4 and low-temperature Gd_5Si_4. For Gd_5Ge_4, the recent paper of Levin *et al* [6] shows the relation between the crystallographic and magnetic transitions induced by temperature and/or magnetic field. The difference between these structures comes from the fact that in Gd_5Ge_4 one of the Ge atomic positions loses the other Ge atom as a nearest neighbour but the symmetry remains unchanged through the transition.

The UPS spectra for three compounds and Gd are shown in figure 2. Generally, the shapes of the spectra are similar to those obtained in the XPS regime. The states which are situated

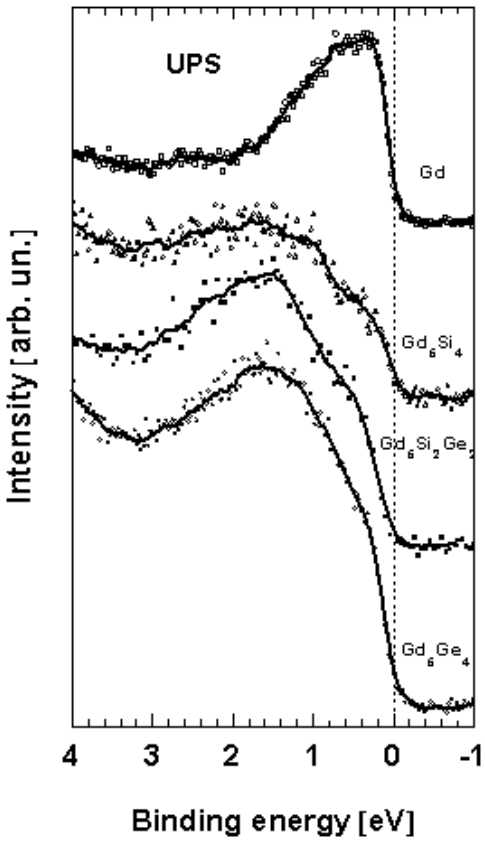

Figure 2. Valence band UPS spectra for Gd_5Si_4, $Gd_5Si_2Ge_2$, Gd_5Ge_4 compounds and the Gd pure element.

just below the Fermi level are more pronounced. This may be related to the increase in the photo-ionization cross-sections with decrease of the photon energy—which is stronger for Gd 5d states than for other valence states [13].

Figures 3–6 show the XPS and UPS spectra obtained for various temperatures. The aim of these measurements was to check whether the electronic structure changes when the magnetic ordering or crystallographic transition takes place. For Gd_5Si_4 (figure 3) a slight difference is visible between the spectra obtained below (298 K) and above (431 K) the Curie point. A decrease in the intensity at a BE of 0.8 eV with increase of the temperature may be related to some changes due to the exchange splitting of the 5d band which is clearly visible in the calculated spin-dependent DOS. The decrease of the exchange splitting above the Curie point may lead to pronounced changes of the total DOS mostly in the energy region characterized by the large slope of the DOS curve, so mainly in the energy region below 1 eV. The observed effect is at a BE beyond the Fermi cut-off even when one takes into account the experimental energy broadening, which is about 0.3 eV.

The temperature dependence of the XPS spectra of $Gd_5Si_2Ge_2$ is shown in figure 4. The spectra were measured for three temperatures: 233, 303 and 473 K. $Gd_5Si_2Ge_2$ exhibits two magnetic transitions: a second-order phase transition from paramagnet to ferromagnet I at $T_C^{\mathrm{I}} = 299$ K and a first-order phase transition from ferromagnet I to ferromagnet II at

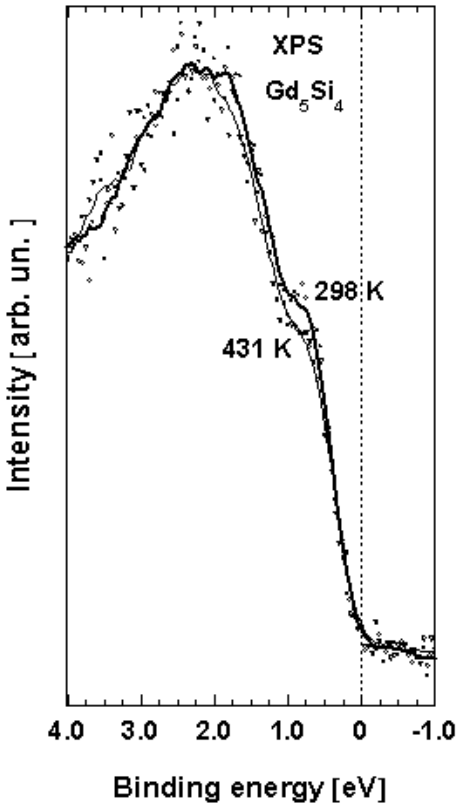

Figure 3. XPS spectra of Gd_5Si_4 at 298 and 431 K.

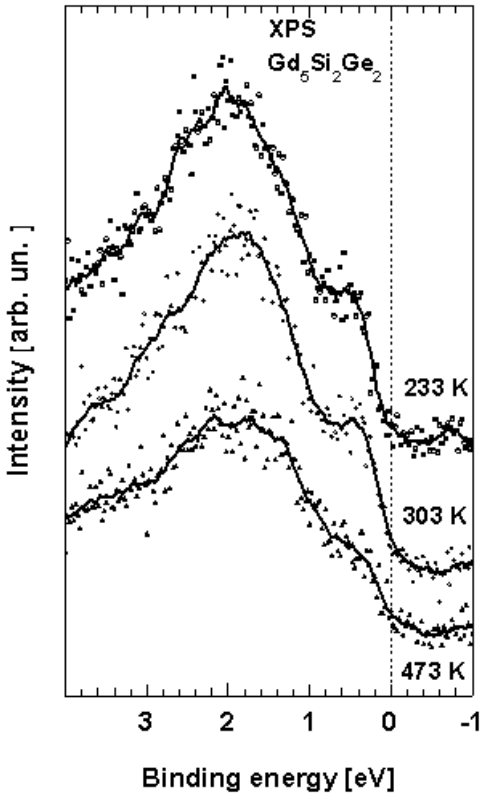

Figure 4. XPS spectra of $Gd_5Si_2Ge_2$ at 233, 303 and 473 K.

$T_C^{\mathrm{II}} = 276$ K [3]. The characteristic peak at about 0.5 eV is much more pronounced for temperatures below T_C, whereas there is no clear difference between the spectra obtained at 303 and 233 K, so above and below the second transition. The main peak at about 2 eV also shows some broadening at 473 K in relation to the spectra obtained in the ferromagnetic region. The observed behaviour is probably connected to the temperature-dependent exchange splitting of the Gd 5d band.

The characteristic transition temperatures for Gd_5Ge_4 are below the cooling limit of our XPS spectrometer, but a slight change in the spectra can be noted when the temperature is lowered to 166 K (figure 5). The bump visible at BE of 0.5–0.8 eV shifts towards the Fermi level for decreasing temperature. One may suppose it to have some relation with the drastic change of the temperature dependence of the electrical resistivity of Gd_5Ge_4 which takes place at 115 or 130 K [5, 6].

The influence of 5 at.% substitution of titanium for Si or Ge has been investigated with respect to the electrical and magnetic properties and electronic structure. The findings for the former will be published elsewhere. XPS and UPS valence band spectra of Gd_5Si_4 and $Gd_5Si_{3.8}Ti_{0.2}$ are presented in figures 6 and 7. A comparison between the spectra of Gd_5Si_4 and $Gd_5Si_{3.8}Ti_{0.2}$ gives information about the energy positions of Ti 3d states. Both XPS and UPS results show a relative increase in photoemission intensity in the vicinity of the Fermi level for Ti-doped compounds. The bump at about 0.5 eV is much more pronounced for $Gd_5Si_{3.8}Ti_{0.2}$.

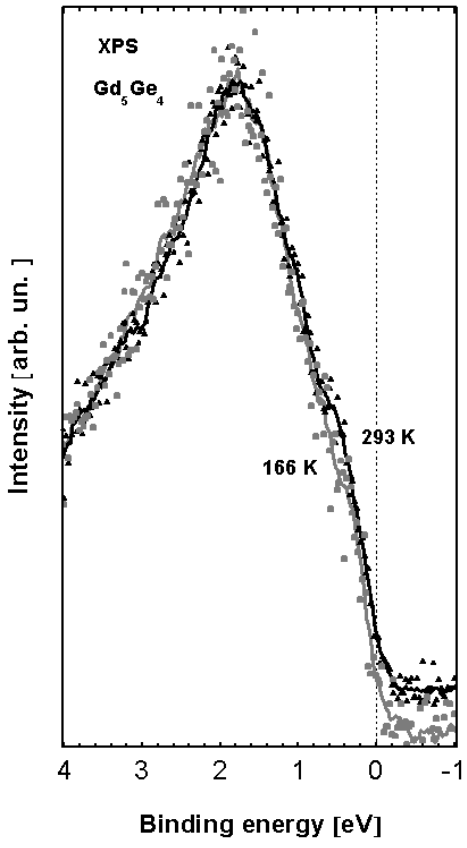

Figure 5. XPS spectra of Gd_5Ge_4 at 166 and 293 K.

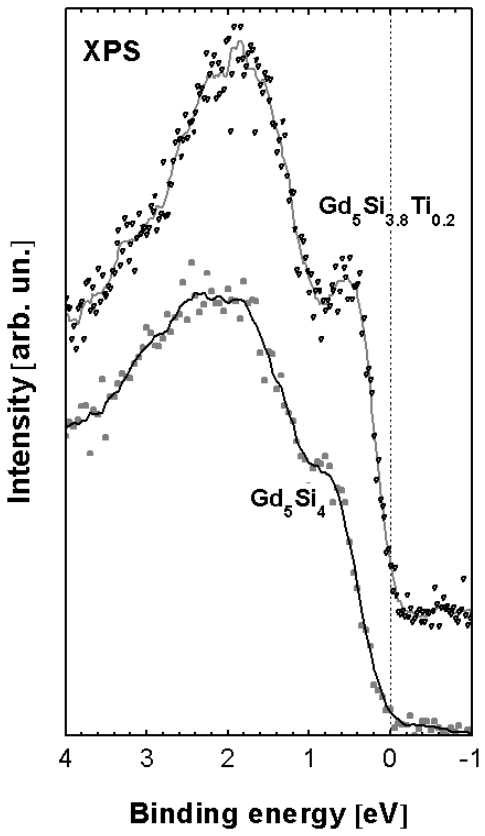

Figure 6. XPS valence band spectra of Gd_5Si_4 and $Gd_5Si_{3.8}Ti_{0.2}$.

This effect may be related to the observed change in character of the electrical resistivity. Similar effects have been observed for $Gd_5Ge_{3.8}Ti_{0.2}$ where a clear increase of the DOS in the region close to the Fermi edge is visible, especially in the UPS spectrum (figure 8). The occurrence of the Ti 3d states near the Fermi level may explain the drastic changes in electrical resistivity and magnetic susceptibility of $Gd_5Ge_{3.8}Ti_{0.2}$ with respect to Gd_5Ge_4.

The chemical shift of the most pronounced photoemission lines has been analysed. The positions of core levels and Gd 4f levels have been compared with the BEs obtained for pure elements using the same spectrometer. Table 1 shows the chemical shifts for the compounds investigated. For all compounds the position of the Gd photoemission peaks is shifted to higher BE, in relation to Gd metal. For Si and Ge levels we observed a negative chemical shift. A positive shift has been observed for the Ti $2p_{3/2}$ level. The chemical shift may be related to the inter-atomic charge transfer or intra-atomic electronic state conversion. Further discussion of the shifts is given below in the context of the electronic structure results.

3.2. Calculations

Figure 9 illustrates the parts of the band structures of Gd_5Si_4 and Gd_5Ge_4 located in the vicinity of the Fermi energy. For Gd_5Si_4, both spin spectra show a narrow energy gap of $\sim$0.05 eV

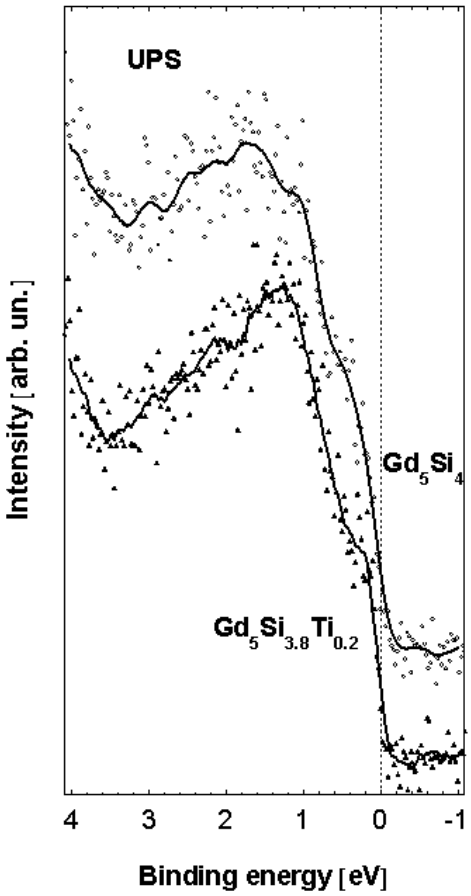

Figure 7. UPS valence band spectra of Gd_5Si_4 and $Gd_5Si_{3.8}Ti_{0.2}$.

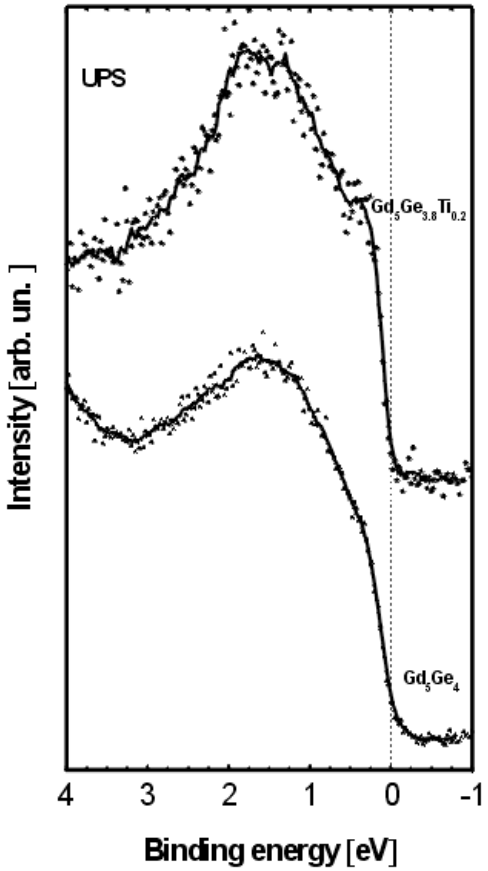

Figure 8. UPS valence band spectra of Gd_5Ge_4 and $Gd_5Ge_{3.8}Ti_{0.2}$.

Table 1. Chemical shifts of most pronounced photoemission levels for Gd_5Si_4, $Gd_5Si_2Ge_2$, Gd_5Ge_4, $Gd_5Si_{3.8}Ti_{0.2}$ and $Gd_5Ge_{3.8}Ti_{0.2}$ compounds. The first row shows the BEs for pure elements (all data are in electron volts).

	Gd 4f, 8.1	Gd $3d_{5/2}$, 1187.0	Si 2p, 99.3	Si 2s, 150.2	Ge 3d, 29.4	Ge 3s, 181.2	Ge $3p_{1/2}$, 125.7	Ti $2p_{3/2}$, 453.9
Gd_5Si_4	+0.1	+0.3	−0.5	−0.25	—	—	—	—
$Gd_5Si_{3.8}Ti_{0.2}$	+0.3	+0.2	−0.1	−0.4	—	—	—	+0.5
Gd_5Ge_4	+0.5	—	—	—	−0.85	−0.7	−0.9	—
$Gd_5Ge_{3.8}Ti_{0.2}$	+0.6	+0.2	—	—	−0.7	−0.4	−0.4	+0.8
$Gd_5Si_2Ge_2$	+0.3	—	−0.4	−0.35	−0.8	−0.7	−0.8	—

width, located at 0.3 eV (minority spin) and 0.7 eV (majority spin) below the Fermi energy. The gap lies within a wider energy region (of 0.5 eV width) with almost no energy states and with only a few energy bands, becoming closer on the R–U line of the BZ forming the narrow gap. A wide pseudo-gap separates the lower-lying hybridized complex of Si p and Gd d bands from the relatively narrow 5d band of Gd. For the Gd_5Ge_4 compound only the minority-spin bands display a narrow pseudo-gap just below the Fermi energy. The minority-spin d states

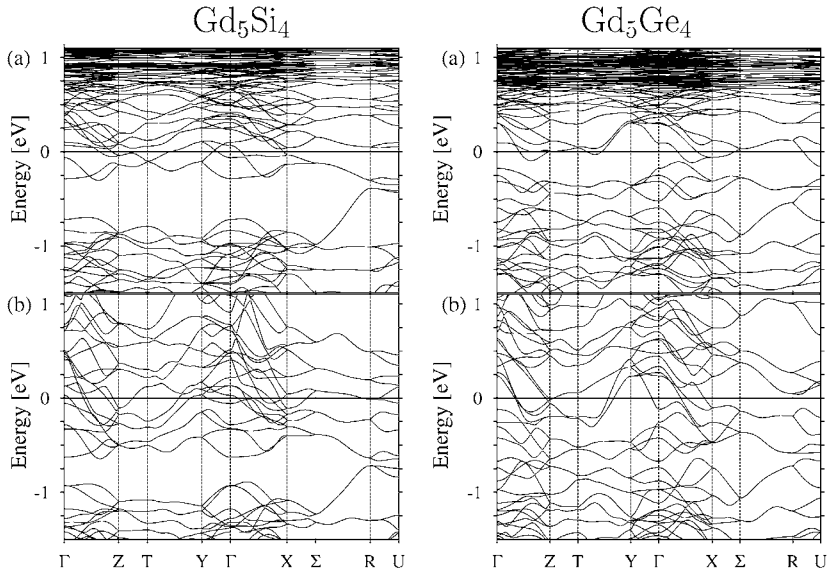

Figure 9. The electronic band structure in the vicinity of the Fermi energy ($\varepsilon_F = 0$). The top and bottom panels show the minority- and majority-spin energy bands, respectively.

of gadolinium form electron band pockets crossing indirectly on the Γ–X line of the BZ the complex of hybridized Ge p and Gd d minority-spin bands. The majority-spin bands distribute more uniformly in this energy range, but the presence of some flat (dispersionless) energy bands just below ε_F gives rise to sharp structures in the DOS.

Figures 10 and 11 present different contributions to the DOSs of the compounds investigated. Figures 10 show the spin-resolved contributions of different atoms with the s, s + p, s + p + d and f parts represented by separate lines. The bottom panels of figure 10 show the spin-resolved total DOS. Figure 11 gives the total (both spins) DOS together with separated average atomic contributions (left panels) and different orbital contributions (right panels). The shapes of the DOS curves of the Gd_5Ge_4 and Gd_5Si_4 compounds resemble those of the DOSs calculated by Levin *et al* [6] for the Gd_5Ge_4 compound in the different (low- and high-temperature) crystal structures. According to our calculations, the low-lying energy bands (6–10 eV below ε_F) are mainly of s character. The dominant contribution to that part of the spectrum comes from s states of Si (Ge), but the contribution of the p states of Gd atoms is also significant. The part of the DOS extending from 4 eV below ε_F to the energy just below ε_F (i.e. the position of the pseudo-gaps) in Gd_5Si_4 is dominated by p states of Si atoms with a small admixture of the s and d states of Gd atoms. For Gd_5Ge_4 the shape of the DOS in this energy region is also determined by the p states (of Ge), but the contribution of Gd d states is also significant. Above the energies where the gaps (or pseudo-gaps) are located, the DOSs of both compounds are built mainly from d states of Gd atoms. Consequently, the DOSs at the Fermi level for both compounds are dominated by the d states of Gd atoms.

The transport properties of metals are governed by their electronic structure in the energy range of several k_BT around the Fermi energy. For both compounds investigated the main contribution to the DOS near the Fermi energy originates from the d states of gadolinium, but the detailed structure of this part of the DOS changes significantly when the Si atoms are replaced by Ge ones. These changes result from the differences in atomic positions between the unit cells of Gd_5Si_4 and Gd_5Ge_4 compounds. Comparison of our results for Gd_5Si_4 with

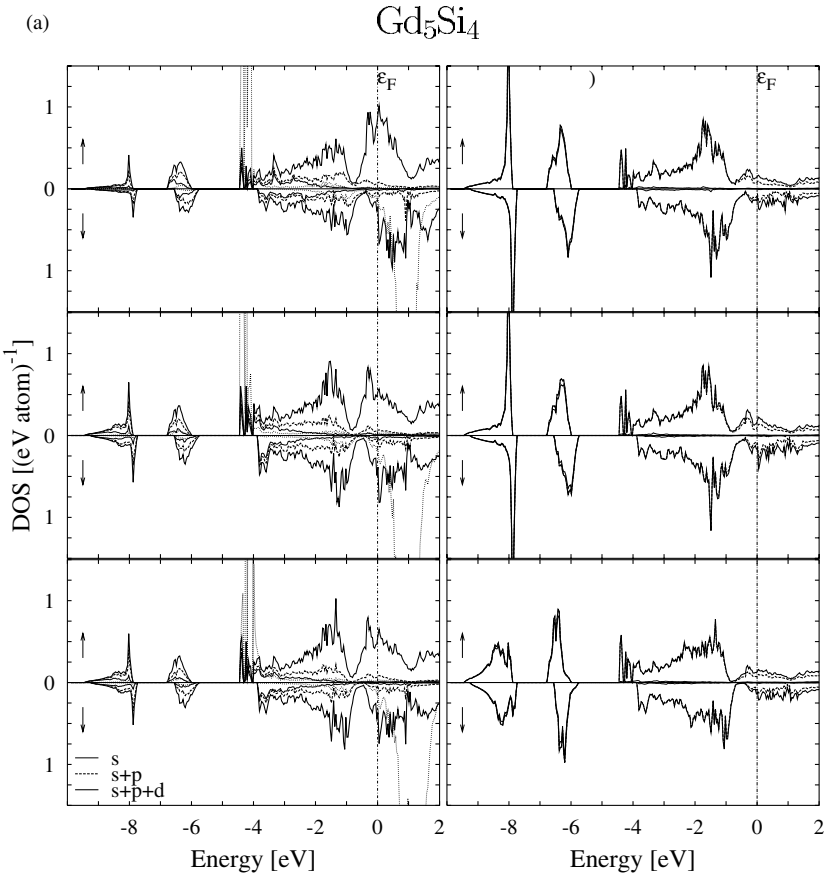

Figure 10. Spin-resolved and orbital-decomposed average atomic DOSs contributed by Gd (a) and metalloid Si, Ge (b) atoms and the total DOSs of Gd_5Si_4 and Gd_5Ge_4. Thin solid, dashed and thick solid curves depict respectively the s, s + p and s + p + d spin DOSs. Thin dotted curves show the 4f DOS at Gd sites. A vertical dashed line in each panel shows the position of ε_F.

the electronic structure of Gd_5Ge_4 (in the crystal structure of Gd_5Si_4 type) calculated by Levin *et al* [6] shows that the differences in electronic structure between Gd_5Ge_4 and Gd_5Si_4 do not depend on the electronic configuration of the metalloid (Si, Ge) atom.

Within the energy range of 1 eV below the Fermi energy, both spin DOSs of Gd_5Si_4 (figure 10) display relatively wide ($\sim$0.2 eV) pseudo-gaps split by the exchange interaction. The positions of the majority-and the minority-spin pseudo-gaps are $\sim$0.8 and 0.5 eV below ε_F, respectively. Above the pseudo-gaps, both spin d states of Gd form the $\sim$2 eV wide band, and the Fermi level is positioned almost in the centre of this band.

Within the same energy range (from ε_F to 1 eV below), each spin electronic structure of Gd_5Ge_4 (figures 10 and 11) consists of a narrow band surrounded by sharp dips. The bands are formed by the 5d states of gadolinium hybridized with the 3p states of germanium. The majority-spin peak is located at 0.5 eV below ε_F, while in the minority-spin spectrum it is shifted by the exchange interaction to lower BEs by 0.15 eV. The dip located on the upper side of the minority-spin narrow band, located at 0.14 eV below ε_F, is significantly wider and forms a pseudo-gap 0.14 eV wide. In the majority-spin spectrum the Fermi level is located within the wide Gd 5d band relatively far above its lower edge, while in the minority-spin spectrum it falls to the lower edge of the 5d Gd band.

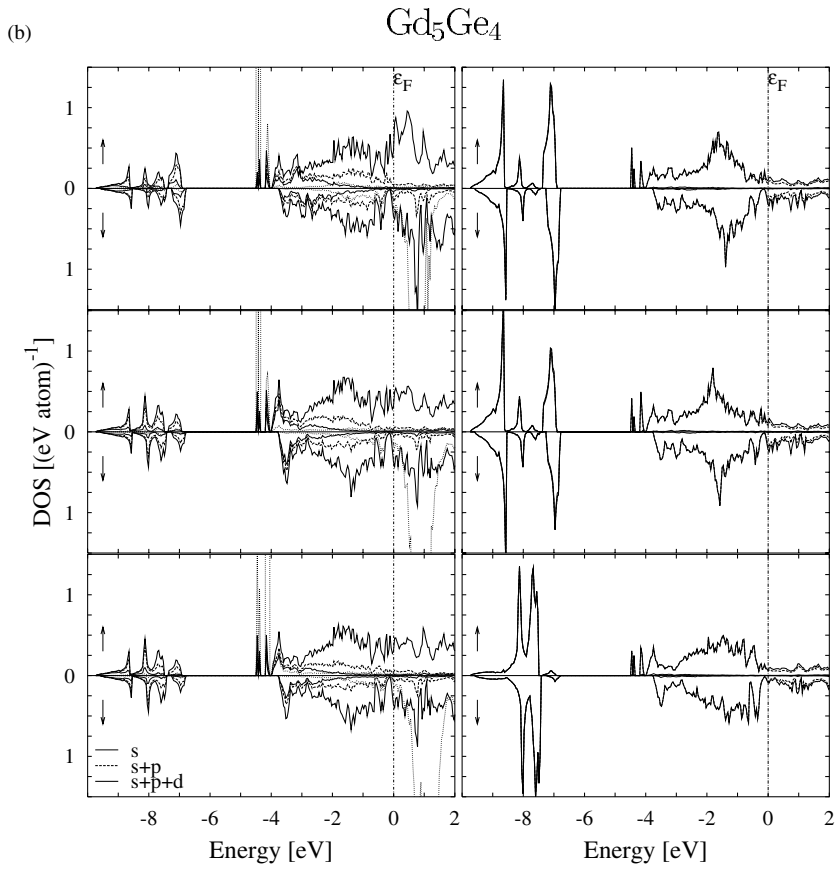

Figure 10. (Continued.)

Analysis of the total DOS curves shown in figure 11 supports the conclusion that the Gd_5Si_4 compound should display metallic electrical transport properties over a wide temperature range. In Gd_5Ge_4 the position of ε_F at the edge of pseudo-gap may give rise to a peculiar variation of the electrical resistivity with temperature. This type of electrical resistivity behaviour, in both compounds, has been confirmed experimentally [5]. The resistivity grows with decreasing temperature down to 115 K [5] or 130 K [6] and then shows metallic behaviour for lower temperatures. Levin *et al* [6] discussed three possible mechanisms of resistivity decrease with increasing temperature. The best fit to the experimental data was obtained with the use of the function $\rho \sim \exp(T_0/T)^{1/4}$ derived from the variable-range hopping (VRH) model [14]. The model assumes Anderson-type localization of electronic states in the vicinity of the Fermi energy. The localization may be caused by magnetic disorder. From the fit of the electrical resistivity to the VRH function the Mott temperature has been found. Using the DOS derived from the electronic heat capacity we have estimated a localization length ξ of 8.3 Å, which corresponds approximately to the unit-cell dimensions. The calculated electronic structure of the Gd_5Ge_4 compound in the non-magnetic state [6] is characterized by a narrow band located at the Fermi level surrounded by small gaps. The localization of the states of this narrow band caused by magnetic disorder above the Curie temperature may give, according to the VRH model, a negative temperature coefficient for the electrical resistivity. Similar behaviour of the electrical resistivity has been observed in $Fe_{2+\varepsilon}V_{1-\varepsilon}Al$ Heusler-type alloys [15]. The

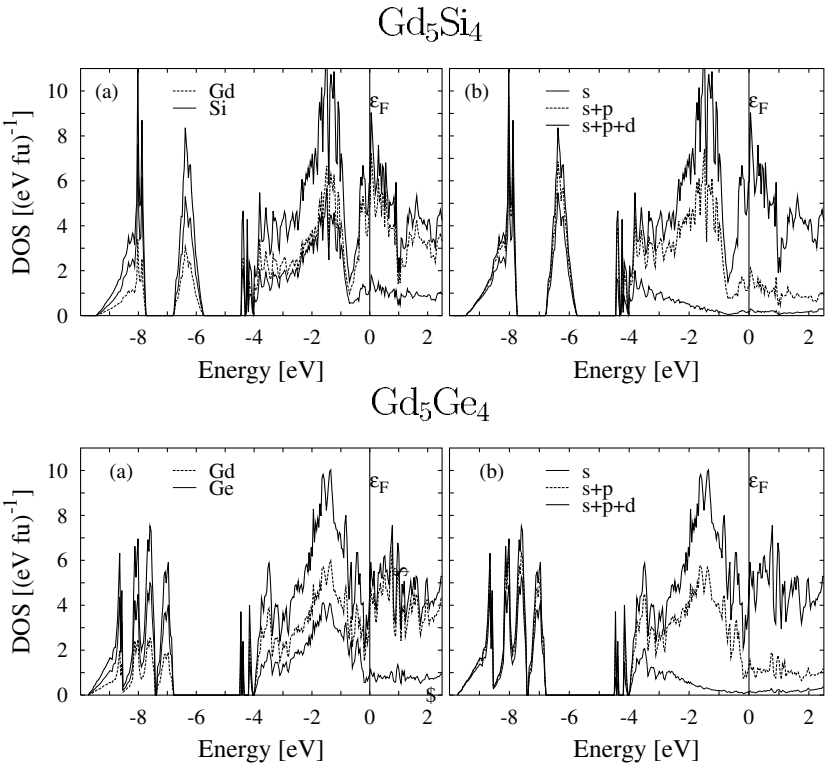

Figure 11. The total spd DOS of Gd_5X_4 (X = Ge, Si) together with separated atomic (a) and orbital (b) contributions. Vertical, dash–dot lines show the position of ε_F.

electronic structure of $Fe_{2+\varepsilon}V_{1-\varepsilon}Al$ ($\varepsilon = 0.06$) in the non-magnetic state also consists of a narrow 3d band located at the Fermi energy separated by gaps or quasi-gaps from the remaining bands [16]. One may suppose that in both systems the magnetic disorder may cause Anderson localization of the electronic states of a narrow band located at the Fermi energy, and as a result the decrease in the electrical resistivity with increasing temperature observed in the paramagnetic state.

Figure 12 shows the XPS and UPS spectra simulated on the basis of the calculated partial densities of states (PDOS). The data for the plots were prepared by convolution of the PDOS with Lorentz functions (with half-widths of 0.35 and 0.2 eV for XPS and UPS, respectively) and multiplication by the corresponding cross-sections taken from [13]. The calculated spectra agree qualitatively with the experimental ones.

For the Gd_5Si_4 compound the calculated XPS and UPS spectra each consist of two features located at BEs of 1.5 and 0.25 eV. The valleys of low intensity visible in both calculated (XPS, UPS) spectra are due to the presence of the energy gap in the DOS of this compound (figure 11). The main contribution to the simulated spectra comes from the d states of gadolinium. The valence states of silicon atoms give a rather small contribution, and that only in the higher BE range (1–4 eV). In the room temperature experimental XPS and UPS spectra of Gd_5Si_4 there exists a bump which can be related to the upper feature of the calculated spectra. Its location in the experimental spectra is not unique. According to the XPS measurements the location of the bump is at a BE of ∼0.8 eV, but in the UPS spectrum it is visible at a BE of 0.3–0.4 eV. The positions of the maxima of the experimental XPS and UPS spectra are the same as those for the calculated ones.

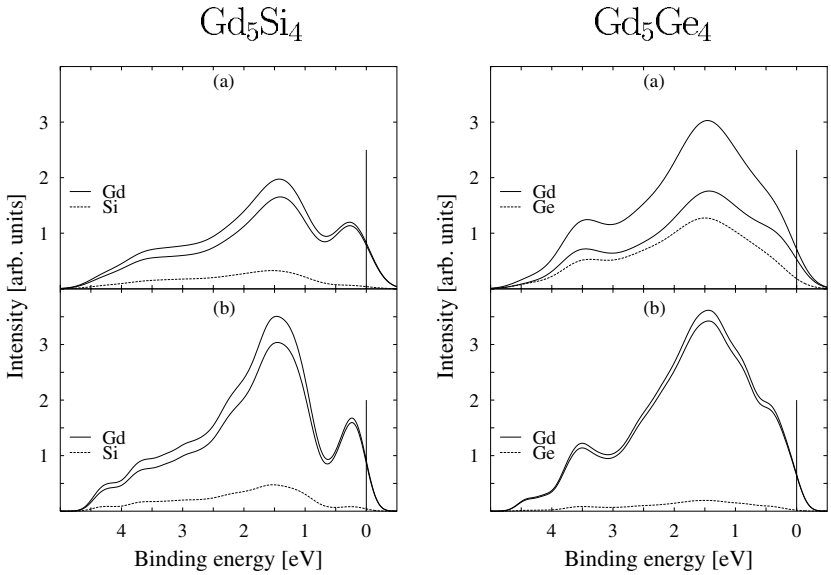

Figure 12. Simulated XPS (a) and UPS (b) spectra of Gd_5X_4 (X = Ge, Si) together with separated atomic contributions.

The calculated XPS and UPS spectra of Gd_5Ge_4 at small BE (0–3 eV) show a broad line with a maximum at ∼1.5 eV and a bump at ∼0.4 eV. The bump, in both spectra, is a result of a sharp dip in the DOS of Gd_5Ge_4 (figure 11) located just below ε_F and is also visible in the UPS spectrum obtained experimentally. The poorer energy resolution and lower Gd 5d sensitivity factor cause the bump to be less visible in the XPS measurement results. The feature located at a BE of ∼3.5 eV in the calculated XPS and UPS spectra comes from the sp states of Ge and can also be confirmed from an upturn in the measured XPS and UPS spectra of Gd_5Ge_4 in the same energy range.

Table 2 summarizes the quantitative results of our band-structure calculations for Gd_5Si_4 and Gd_5Ge_4. The magnetic data can be summarized as follows. In both compounds, the atomic magnetic moment of gadolinium is slightly reduced as compared with that of gadolinium in its elemental hcp structure. This effect results from the reduction of the magnetic polarization of the 5d bands. The reduction is more significant in the Gd_5Ge_4 compound, where on average the 5d magnetic moment of Gd atoms is less than that in the hcp Gd by 0.17 μ_B [16]. For the Gd_5Si_4 compound the magnitude of the 5d magnetic moment of Gd atoms is on average higher by ∼0.09 μ_B than for Gd_5Ge_4 but still lower than that for elemental hcp Gd. The calculations have shown that in the compounds the magnetic polarization of the s–p bands is also strongly reduced. In hcp Gd the s–p bands give a contribution of ∼0.25 μ_B [17], while in the Gd_5Ge_4 and Gd_5Si_4 compounds the magnetic moment contributed by s–p bands is vanishingly small (∼0.07 μ_B, on average).

For the compounds investigated the magnitudes of the localized 4f moments of Gd atoms are similar to those for hcp Gd and are less than the atomic value (7 μ_B) because of the presence at the Fermi surface of minority-spin 4f bands giving a non-vanishing 4f PDOS at and just below ε_F. It should be noted that the presence of the minority 4f states at the Fermi level may be a result of the LSDA approach used in the calculations. The average magnetic moment (per Gd atom) equals 7.27 and 7.13 μ_B for Gd_5Si_4 and Gd_5Ge_4, respectively, and the corresponding reductions with respect to hcp Gd are 0.28 and 0.42 μ_B.

Table 2. Partial atomic occupations n, magnetic moments μ (μ_B/atom) and DOSs at the Fermi energy $D(\varepsilon_F)$ (eV^{-1}/atom), with separated orbital contributions (s + p, d and f). Values of the total magnetic moment (μ_{tot}) and the total DOS ($D_{tot}(\varepsilon_F)$) are given per formula unit.

			μ (μ_B/atom)				$D(\varepsilon_F)$ (eV^{-1}/atom))		
		ΔQ	s + p	d	f	Total	s + p	d	f
Gd_5Si_4	Gd_1 4(c)	−0.06	0.09	0.39	6.85	7.33	0.11	0.87	0.13
	Gd_2 8(d)	0.65	0.07	0.31	6.87	7.25	0.23	1.46	0.37
	Gd_3 8(d)	0.27	0.07	0.29	6.88	7.24	0.23	1.46	0.29
	Si_1 4(c)	−0.37	−0.04	0.03	—	−0.01	0.15	0.09	—
	Si_2 4(c)	−0.47	−0.01	0.03	—	0.02	0.17	0.12	—
	Si_3 8(d)	−0.67	−0.04	0.03	—	−0.01	0.31	0.17	—
	$\mu_{tot} = 36.3\ \mu_B$/fu,				$D^{\uparrow}_{tot}(\varepsilon_F) = 3.28\ eV^{-1}$/fu				
	$\langle\mu_{Gd}\rangle = 7.27\ \mu_B$/atom				$D^{\downarrow}_{tot}(\varepsilon_F) = 2.92\ eV^{-1}$/fu				
Gd_5Ge_4	Gd_1 4(c)	0.41	0.09	0.25	6.84	7.18	0.17	0.64	0.27
	Gd_2 8(d)	0.67	0.04	0.24	6.85	7.13	0.15	1.29	0.40
	Gd_3 8(d)	0.37	0.05	0.22	6.86	7.13	0.22	1.14	0.28
	Ge_1 4(c)	−0.55	−0.03	0.02	—	−0.01	0.23	0.08	—
	Ge_2 4(c)	−0.52	−0.02	0.02	—	—	0.25	0.08	—
	Ge_3 8(d)	−0.71	−0.05	0.01	—	−0.04	0.26	0.06	—
	$\mu_{tot} = 35.6\ \mu_B$/fu				$D^{\uparrow}_{tot}(\varepsilon_F) = 2.13\ eV^{-1}$/fu				
	$\langle\mu_{Gd}\rangle = 7.13\ \mu_B$/atom				$D^{\downarrow}_{tot}(\varepsilon_F) = 3.43\ eV^{-1}$/fu				

The total DOSs in Gd_5Si_4 and Gd_5Ge_4 averaged per Gd atom are 1.24 and 1.11 eV^{-1}/atom, respectively. These values are much smaller than the calculated total DOSs of hcp Gd.

Table 2 presents the charge transfers (ΔQ) for different constituent atoms. In the ASA-based calculations the magnitudes of the charge transfers depend on the choice of WS radii and cannot be treated rigorously. Nevertheless, some conclusions concerning the tendency of flow of the electronic charge within the unit cell can be drawn from the ASA calculations. For both compounds investigated the calculations have shown a tendency for gadolinium atoms to gain some proportion of electrons at the cost of metalloid atoms. This result contradicts the experimentally observed chemical shift of the 4f and core levels of Gd to higher BEs with respect to their positions for hcp Gd. However, the detailed analyses of the partial populations of the s, p and d valence states have shown that, despite the increase in the number of electrons on the Gd atoms, the population of the 6s states is reduced as compared to that on Gd atoms in the hcp structure. This may indicate that the intra-atomic charge transfer takes place on the Gd atoms. Reduction of the number of 6s-type electrons, which have the opportunity to come closer to the nuclei than the core shell-4 and shell-5 electrons, can diminish the screening and produce a chemical shift of core levels to higher BEs.

4. Conclusions

Comparison between the calculated and experimental electronic structures indicates a very good agreement. The results obtained with the TB-LMTO method have also given us the opportunity to explain the observed resistivity and magnetic behaviour. The energy gaps have been found for both compounds. For Gd_5Si_4 the gap is situated below the Fermi level and does not influence the resistivity. For Gd_5Ge_4 the gap is responsible for the semiconducting-like behaviour of the resistivity for temperatures above 115 K. Our results for Gd_5Ge_4 are in agreement with recent data published by Levin *et al* [6]. The different properties of the isostructural

Gd_5Si_4 and Gd_5Ge_4 compounds are reflected in the different shapes of the DOSs in the energy region between 0 and −1 eV. Moreover, the observed temperature dependence of the XPS and UPS spectra in the region close to the Fermi region has been related to the details of the calculated electronic structure.

The calculations have confirmed the conclusion from our earlier paper [5] that the 5d character of the valence electrons determines the most important properties of both compounds. The high ferromagnetic ordering temperature may be understood as a result of the high density of the d states, which are strongly polarized and mediate the exchange interaction between the 4f magnetic moments.

References

[1] Pecharsky V K and Gschneidner K A Jr 1997 *Phys. Rev. Lett.* **78** 4494
[2] Pecharsky V K and Gschneidner K A Jr 1997 *Appl. Phys. Lett.* **70** 3299
[3] Pecharsky V K and Gschneidner K A Jr 1997 *J. Magn. Magn. Mater.* **167** L179
[4] Levin E M, Pecharsky V K and Gschneidner K A Jr 2001 *Phys. Rev.* B **63** 174110
[5] Szade J and Skorek G 1999 *J. Magn. Magn. Mater.* **196–7** 699
[6] Levin E M, Pecharsky V K, Gschneidner K A Jr and Miller G J 2001 *Phys. Rev.* B **64** 235103
[7] Morellon L, Blasco J, Algarabel P A and Ibarra M R 2000 *Phys. Rev.* B **62** 1022
[8] Levin E M, Pecharsky V K and Gschneidner K A Jr 1999 *Phys. Rev.* B **60** 7993
[9] Andersen O K and Jepsen O 1984 *Phys. Rev. Lett.* **53** 2571
Andersen O K, Jepsen O and Glötzel D 1985 *Highlights of Condensed Matter Theory* ed F Bassani, F Fumi and M P Tosi (Amsterdam: North-Holland) p 59
Jepsen O and Andersen O K 1971 *Solid State Commun.* **9** 1763
[10] von Barth V and Hedin L 1972 *J. Phys. C: Solid State Phys.* **5** 1629
[11] Langreth D C and Mehl M J 1981 *Phys. Rev.* B **28** 1809
Hu C D and Langreth D C 1985 *Phys. Scr.* **32** 391
[12] Pecharsky V K and Gschneidner K A Jr 1997 *J. Alloys Compounds* **260** 98
[13] Yeh J and Lindau I 1985 *At. Data Nucl. Data Tables* **32** 1
[14] Mott N F 1974 *Metal–Insulator Transitions* (London: Taylor and Francis) p 278
[15] Kato M, Nishino Y, Mizutani U and Asano S 2000 *J. Phys.: Condens. Matter* **12** 1769
[16] Deniszczyk J 2001 *Acta Phys. Pol.* B **32** 529
[17] Skorek G, Deniszczyk J, Szade J and Tyszka B 2001 *J. Phys.: Condens. Matter* **13** 6397